CENTER OF EXCELLENCE FOR AIRPORT TECHNOLOGY

TECHNICAL NOTE

TECH NOTE NO:	32
TITLE:	Moisture and Temperature Curling Stresses in Airfield Concrete Pavements
AUTHORS:	Robert Rodden, Drs. J. Roesler & D. Lange
	Ph: (217) 265-0218, Email: jroesler@uiuc.edu
CONTACT:	University of Illinois, Dept of Civil & Environmental Engineering 1211 NCEL, MC-250, Urbana, IL 61801
DATE/REV:	12/05/2006

EXECUTIVE SUMMARY

Temperature and moisture gradients can cause significant tensile stresses in concrete pavement, which can lead to cracking without application of any mechanical loads. Currently, most analysis and design methods assume linear distribution of thermal and hygrothermal strains through the slab depth, which usually underestimates the critical tensile stresses in the concrete pavement. A micromechanical approach to calculate the moisture curling stresses in concrete pavements based on measured relative humidity gradients is proposed. In this approach, the loss in moisture from the cement microstructure creates a negative pressure in the concrete capillary pores, which ultimately produces the bulk concrete shrinkage and moisture curling (differential shrinkage). The hygrothermal strain at each point in the slab depth is calculated through the Kelvin-Laplace and Mackenzie equations, which provide a basis for calculating the moisture curling stresses at any time, similarly to the formulation for calculating temperature curling stresses. The evolution of stresses due to nonlinear temperature and moisture gradients are calculated based on field measurements with consideration for the tensile creep of concrete. The proposed formulation allows for a concise analytical solution to evaluate the effects of slab size and the concrete's material constituents on moisture and temperature curling stresses.

INTRODUCTION

The design of concrete structures is primarily based on the dead and live loading. The importance of environmental loading is often diminished in concrete structures due to the complicated interaction of the structures geometry, materials, and time dependency of the environmental loading and material properties. Even with advances in high-performance concretes and mineral and chemical admixtures, concrete pavements periodically exhibit early age cracking due to environmental loading alone. A concrete slab cracks due to environmental stresses typically in the early stages of hydration when the concrete is still developing the strength and fracture toughness necessary to resist the resultant stresses from the environment. Thus, early age temperature and relative humidity (RH) profile measurements are critical when attempting to predict the cracking of the slab.

Environmental loading consists of thermal strains – resulting from a thermal differential between the surface and base of the slab and the temperature difference between the slab's zero stress temperature and the current temperature – and hygrothermal strains – resulting from a RH differential between the surface and base of the slab. If a slab were weightless and unrestrained, then the resulting deflections due to temperature and RH could occur without generation of internal stresses. The self-weight of the slab, however, provides restraint causing any environmentally-induced strain to produce a corresponding stress. In addition to the two thermal and hygrothermal stresses, tensile creep (relaxation) is also present, which reduces the environmentally-developed stresses by some percentage.

Currently, most analysis and design methods assume a linear distribution through the slab depth for the thermal and hygrothermal strains, which usually underestimates the critical tensile stresses in the concrete pavement. This paper will present the environmental stresses due to non-linear thermal and moisture curling based on a micromechanical model for a single concrete slab fully supported.

TENSILE STRESS COMPONENTS

The tensile stress in the interior of a concrete slab as a result of temperature curling [Westergaard 1927] is

$$\sigma = \frac{E\varepsilon_{tot}}{2(1-\nu)} \qquad (1)$$

where σ = tensile stress; E = modulus of elasticity; ε_{tot} = total strain; and ν = Poisson's ratio. As this Westergaard solution is for an infinitely long slab, Bradbury implemented a correction factor to the Westergaard solution for slabs of finite dimensions. When the slab is close to square, which will be assumed for this analysis, the tensile stress becomes

$$\sigma = \frac{CE\varepsilon_{tot}}{2(1-\nu)} \qquad (2)$$

where C = Bradbury coefficient. Typical values of C are less than 1.0 and range from 0.6-0.9 [ERES 2004].

The total strain in the slab can be rewritten in its component form

$$\varepsilon_{tot} = \varepsilon_T + \varepsilon_{HT} + \varepsilon_{CR} \tag{3}$$

in which ε_T = thermal strain (curling); ε_{HT} = hygrothermal strain (warping); and ε_{CR} = creep strain (relaxation).

In order to accurately calculate creep strain a complete stress history must be known. Field slabs undergo daily cyclical stresses that are non-uniform with slab depth and change with increasing hydration products. Current creep models are primarily based on uniaxial stress states in controlled environments. It has been found that creep relaxes the restrained shrinkage strain by approximately 50% for both normal and high strength concretes [Altoubat 2000]. Thus, to overcome any difficulties with creep, a 50 percent creep relaxation with respect to free drying shrinkage is proposed, making the total strain

$$\varepsilon_{tot} = \varepsilon_T + 0.5 \cdot \varepsilon_{HT} \,. \tag{4}$$

Although this oversimplifies the creep component and its interaction with the thermal and hygrothermal strain calculations, it is currently necessary for completion of the analytical model. The tensile stress in a concrete slab generalized at any point in the cross section and at any time becomes

$$\sigma(t,z) = \frac{C(t)E(t)\varepsilon(z)}{2(1-\nu)} = \frac{C(t)E(t)\left(\varepsilon_T(t,z) + 0.5 \cdot \varepsilon_{HT}(t,z)\right)}{2(1-\nu)} \tag{5}$$

where z = distance from the slab's mid-depth with positive z pointing towards the base. Since the goal of this study is to quantify only the total linear and nonlinear stresses in the rigid pavement system (ignore the axial stresses generated by friction), the total linear and nonlinear tensile stress can be rewritten as its component of the total tensile stress

$$\sigma_{L+NL}(t,z) = \frac{C(t)E(t)\left(\varepsilon_{T_{L+NL}}(t,z) + 0.5 \cdot \varepsilon_{HT_{L+NL}}(t,z)\right)}{2(1-\nu)} \,. \tag{6}$$

THERMAL STRAIN

The thermal strain in a concrete material is generalized as

$$\varepsilon_T = \alpha_t \cdot \Delta T \tag{7}$$

where ε_T = thermal strain; α_t = coefficient of thermal expansion; and ΔT = temperature difference. In many cases the actual temperature profile is decomposed into an equivalent linear temperature difference, ΔT [ERES 2004, Jeong 2005]. Ignoring the nonlinear temperature stresses can overestimate the maximum daytime stress by 11-15% and underestimate the nighttime stress by 6-19% [Choubane 1995] or more [Mohamed 1997]. Furthermore, without a reference or set temperature, axially-generated thermal stresses cannot be calculated. To overcome such difficulties and potential inaccuracies, the analysis presented herein uses the set temperature as the basis, making the thermal strain

$$\varepsilon_T = \alpha_t \cdot (T - T_{set}) \tag{8}$$

where T = current temperature and T_{set} = set temperature, respectively. Proposed values for T_{set}, based on a percentage of the peak hydration temperature during hydration, are available elsewhere [Kohler 2005, Schindler 2002].

The thermal strain at any point in the cross section becomes

$$\varepsilon_T(z) = \alpha_t (T(z) - T_{set}(z))\,. \tag{9}$$

A third degree polynomial function was used to model the temperature profile at both the time of set and any time thereafter such that

$$\begin{aligned} T(z) - T_{set}(z) &= (A + Bz + Cz^2 + Dz^3) - (E + Fz + Gz^2 + Hz^3) \\ T(z) - T_{set}(z) &= T_A + T_L(z) + T_{NL}(z) \end{aligned} \tag{10}$$

where A, B, C, and D = regression coefficients for the $T(z)$ fit; E, F, G, and H = regression coefficients for the $T_{set}(z)$ fit; and $T_A(z)$, $T_L(z)$, and $T_{NL}(z)$ = the axial, linear, and nonlinear components of the temperature difference profile.

The axial portion of the total temperature stress can then be solved for as

$$T_A(z) = \int_{-h/2}^{h/2} \frac{T(z) - T_{set}(z)}{h} dz = \left(A + \frac{Ch^2}{12} \right) - \left(E + \frac{Gh^2}{12} \right) \tag{11}$$

and then subtracted out of the total thermal strain equation to yield

$$\varepsilon_{T\,L+NL}(z) = \alpha_t \left(\left[Bz + Cz^2 - \frac{Ch^2}{12} + Dz^3 \right] - \left[Fz + Gz^2 - \frac{Gh^2}{12} + Hz^3 \right] \right) \tag{12}$$

the total linear and nonlinear thermal strains at any point in the cross section. The total linear and nonlinear thermal strain can now be applied at any time step especially for early age concrete stress analysis.

HYGROTHERMAL STRAIN

As a concrete slab is subjected to ambient conditions with an RH less than that of the surface of the slab, moisture will diffuse out of the concrete. The lower the ambient condition, the greater the driving force and the lower the internal RH of the concrete will become. This loss of water from hardening concrete is generally referred to as drying shrinkage. It has been found that concrete subjected to daily cycling of RH in the field can approach the same shrinkage level as that caused by complete drying at a constant RH [Neville 1996]. Thus, the magnitude of the RH strains can become significantly greater than the thermal strains and may result in a permanent concave shape for the slab. Cracks may then initiate at the surface of the slab due to environmental loading and the likelihood of surface-initiated cracks from mechanical loads is increased.

The hygrothermal strain has been quantified using an equivalent humidity difference coefficient, $\Delta[1-(RH)^3]_{eq}$, with respect to the bottom of the slab [ERES 2004, Jeong 2005, Mohamad 1997]. While this formulation allows for a closed form solution of the equivalent linear hygrothermal stresses, the formula was originally intended for calculating the average drying shrinkage of a cross-section subjected to a constant RH environment. Since the effect of moisture gradients on curling is the objective, a micromechanical model is proposed which allows for calculation of both the linear and nonlinear hygrothermal strain at any time increment without knowledge of the concrete's ultimate shrinkage strain.
To solve for hygrothermal strains, the Kelvin Equation is first employed

$$p = \frac{2\gamma}{r} = \frac{\ln(RH)RT}{v_w} \tag{13}$$

where p = average hydrostatic (internal) pressure; RH = relative humidity; R = universal gas constant; T = temperature; and v_m = molar volume of water [Defray 1966, Bentz 1998, Grasley 2003]. As the internal RH decreases in a sealed system with capillary-size pores, the average hydrostatic pressure decreases (underpressure) in the pores due to the pore's radius of curvature decreasing [Grasley 2003]. To solve for hygrothermal strains in terms of pore pressure, the Mackenzie's Equation is used which relates the bulk strain in an elastic media to the internal pressure exerted in circular pores

$$\varepsilon_{HT} = p\left[\frac{1}{3k} - \frac{1}{3k_0}\right] \tag{14}$$

where ε_{HT} = strain caused by drying-induced capillary pressure; k = bulk modulus of the porous solid; and k_0 = bulk modulus of the solid skeleton material [Mackenzie 1950]. As this equation is only completely applicable to saturated solids containing spherical holes, Bentz *et al.* suggested inclusion of a saturation factor in order to consider partially saturated cement paste [Bentz 1998]

$$S = 1 - 0.75\left[1 - \left(\frac{RH}{0.98}\right)^3\right] \text{ valid from 25\% to 98\% RH} \tag{15}$$

making the hygrothermal strain equation

$$\varepsilon_{HT} = S \cdot p\left[\frac{1}{3k} - \frac{1}{3k_0}\right]. \tag{16}$$

Finally, a total shrinkage strain can be derived at any point in the cross section by substituting the Kelvin Equation into the modified Mackenzie's Equation, yielding

$$\varepsilon_{HT}(z)^{Total} = \frac{RT(z)}{v_w}\left[\frac{1}{3k} - \frac{1}{3k_0}\right]\left[1 - 0.75\left[1 - \left(\frac{RH(z)}{0.98}\right)^3\right]\right]\ln(RH(z)) \tag{17}$$

where *T(z)* = same temperature profile as used in the thermal strain calculations and *RH(z)* = relative humidity profile at any given time.

If the average axial hygrothermal strain is calculated and subtracted out as was completed in the above thermal strain calculation, the total linear and nonlinear hygrothermal strain is the following:

$$\varepsilon_{HT\,L+NL}(z) = \varepsilon_{HT}(z)^{Total} - \frac{1}{h}\int_{-h/2}^{h/2}\frac{RT(z)}{v_w}\left[\frac{1}{3k} - \frac{1}{3k_0}\right]\left[1 - 0.75\left[1 - \left(\frac{RH(z)}{0.98}\right)^3\right]\right]\ln(RH(z))dz \tag{18}$$

This equation can again be applied at any time step. The total hygrothermal strain calculation is simple given any measured temperature and RH profile, but the integration of the axial hygrothermal strain requires more manipulation for a concise analytical solution.

Typical RH sensing devices have reasonably high error at RH values greater than 97%, a zone often considered saturated. Field tests have shown that any point deeper than approximately 76.2 mm (3 in.) from the surface of a sufficiently thick slab will remain in this zone [Rodden 2006]. A traditional third order polynomial fit is not representative of such an RH profile. A better fit for a typical RH profile of a relatively thick concrete slab is of the form

$$RH(z) = 1 - \frac{1}{e^{A+Bz+Cz^2+...}} \tag{19}$$

where *A, B, C, etc* = regression coefficients. In order to more easily integrate ln(*RH(z))*, a Taylor series expansion for the natural log of *RH(z)* is needed.

$$\ln(1+x) = \sum_{n=1}^{\infty} \frac{(-1)^{n+1}}{n} \cdot x^n \quad \text{for } |x| < 1 \tag{20}$$

The first two terms of the Taylor series expansion of the ln[*RH(z)*] term can now be written as

$$\ln(RH(z)) = -\frac{1}{e^{A+Bx+Cx^2}} - \frac{1}{2}\left(\frac{1}{e^{2A+2Bx+2Cx^2}}\right) \tag{21}$$

when considering a fit to just three data points. Using just the first two terms of the expansion results in only a 4.5% deviation from the true *RH(z)* value at 65% RH at any depth, with increasing accuracy as the RH increases. With the inclusion of this Taylor series expansion for the natural log, any mathematical processing software can quickly solve a series of time steps of the total linear and nonlinear hygrothermal strain calculation (note that integration can deliver a closed form solution but, for the given assumptions, the results are too length to present herein).

APPLICATION OF MODEL

An example of the combined thermal and hygrothermal stresses are presented below. Data for this example is from a field test of a 381 mm (15 in.) thick slab with 4.57 m (15 ft) slab length and width, cast on October 25, 2005 in Rantoul, Illinois, USA (Rodden 2006). All strain/stress calculations are for the surface (0 mm or 0 in.) as it is assumed that cracking will initiate there. Assumed constants include: C = 0.62, $E = 2.55\text{x}10^4$ MPa, v = 0.2, $\alpha_t = 9\ \text{x}10^{-6}$/°C, R = 8.314 J/mol*K, $k = 1.46 \times 10^{10}$ Pa, $k_0 = 2.6 \times 10^{10}$ Pa, and $v_m = 1.8 \times 10^{-5}$ m^3/mole. The measured temperature and *T(z)* fits for the maximum and minimum thermal stresses occurring during a 24-hour period are shown in Figure 1(a). These temperature profiles are fit to points at 0 mm (0 in.), 25.4 mm (1 in.), 177.8 mm (7 in.), and 355.6 mm (14 in.). The measured RH and RH profile using the Taylor series expansion fit to points at 0 mm (0 in.), 12.7 mm (0.5 in.), and 381 mm (15 in.), with the 381 mm (15 in.) point being assumed to be saturated at 98% RH, are shown in Figure 1(b). Using the temperature and RH fit equations with the formulation presented, the linear and nonlinear thermal, hygrothermal, and total strains can be calculated at each time step (1 hour) and plotted, as shown in Figure 1(c). From the total linear and nonlinear strain, the stress calculation was performed as shown in Figure 1(d).

Despite the linear and nonlinear thermal strain being approximately ± 50 microstrain at early ages, a value also noted elsewhere [Jeong 2005], the total linear and nonlinear strain and resultant stress are both almost always negative or in tension even with a 50% creep relaxation. This behavior is driven by the magnitude of hygrothermal stresses relative to thermal stresses and it exemplifies the importance of accurate hygrothermal strain consideration in modern stress analysis for concrete pavements.

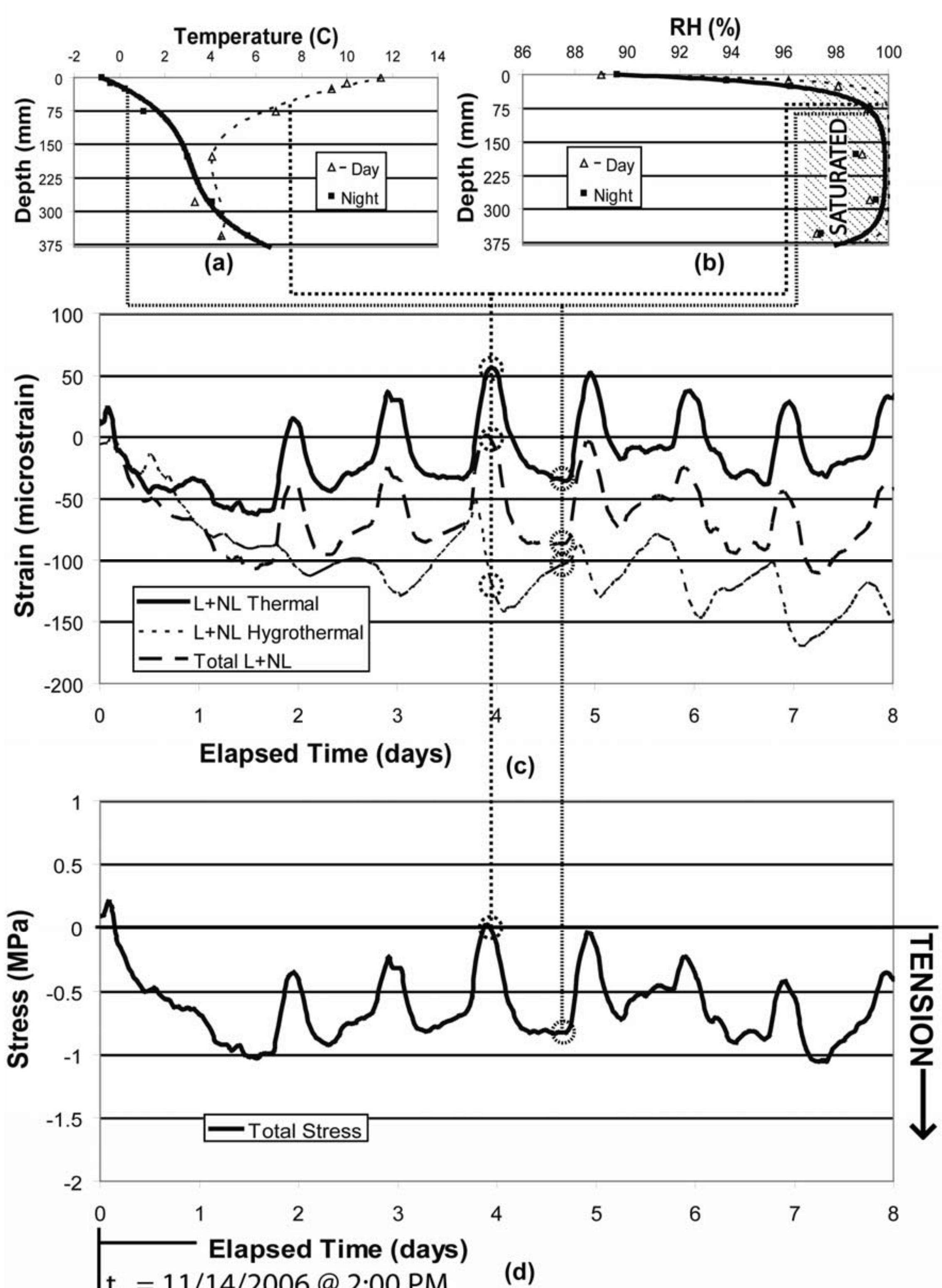

Figure 1. (a) Measured temperature and temperature profiles for day and night fit to data at 0 mm (0 in.), 25.4 mm (1 in.), 177.8 mm (7 in.), and 355.6 mm (14 in.); (b) measured RH and Taylor series fit to data at 0 mm (0 in.), 12.7 mm (0.5 in.), and 381 mm (15 in.) (base assumed to be saturated at 98% RH); (c) linear and nonlinear thermal strain, linear and nonlinear hygrothermal

strain, and total linear and nonlinear strain with creep considered versus time; and (d) total stress versus time.

CONCLUSIONS

A novel micromechanical approach to calculating both the linear and nonlinear moisture curling strains in concrete slabs based on measured relative humidity gradients was presented. In addition to moisture curling considerations, creep relaxation and linear and nonlinear thermal strains were also accounted for in the model. The combined curling stress analysis was applied to temperature and RH profiles measured during an 8 day period in order to calculate the curling stresses at any time increment. This procedure revealed the importance of moisture profile consideration, as it is shown to be a significant factor in the slab's stresses especially at early ages.

REFERENCES

Altoubat, S., "Early Age Stresses and Creep-Shrinkage Interaction of Restrained Concrete", Ph.D. Thesis, University of Illinois at Urbana-Champaign, 2000.

Bazant, Z.P., Murphy, W.P., "Creep and Shrinkage Prediction Model for Analysis and Design of Concrete Structures - Model B3", Materials and Structures 28, July 1995, pp 357-365.

Bentz, D.P., Graboczi, E.J., Quenard, D.A., "Modeling Drying Shrinkage in Reconstructed Porous Materials: Application to Porous Vycor Glass", Modeling and Simulation in Material Science and Engineering 6, 1998, pp 211-236.

Choubane, B., Tia, M., "Analysis and Verification of Thermal-Gradient Effects on Concrete Pavement", Journal of Transportation Engineering 121, 1995, pp 75-81.

Defray, R., Prigogine, I., Bellemans, A., Everett, D.H., "Surface Tension and Absorption", John Wiley & Sons, Inc., New York, 1966.

ERES, "Guide for Mechanistic-Empirical Design of New and Rehabilitated Pavement Structures: Part 3. Design Analysis", ARA, Inc., ERES Consultants Division, May 2004.

Grasley, Z.C., "Internal Relative Humidity, Drying Stress Gradients, and Hygrothermal Dilation of Concrete", M.S. Thesis, University of Illinois at Urbana-Champaign, 2003.

Jeong, J.H., Zollinger, D.G., "Environmental Effects on the Behavior of Jointed Plain Concrete Pavements", Journal of Transportation Engineering, February 2005, pp 140-148.

Kohler, E.R., "Experimental Mechanics of Crack Width in Full-Scale Sections of Continuously Reinforced Concrete Pavements", Ph.D. Thesis, University of Illinois at Urbana-Champaign, 2005.

Mackenzie, J.K., "The Elastic Constants of a Solid Containing Spherical Holes", Proceedings of the Physical Society B63, 1950, pp 1-11.

Mohamed, A.R., Hansen, W., "Effect of Nonlinear Temperature Gradient on Curling Stresses in Concrete Pavements", Transportation Research Record 1568, 1997, pp 65-71.

Neville, A.M. “Properties of Concrete”, 4th Ed., John Wiley & Sons, Inc., New York, 1996.

Rodden, R.A., “Analytical Modeling of Environmental Stresses in Concrete Slabs”, M.S. Thesis, University of Illinois at Urbana-Champaign, 2006.

Schindler, A.K., McCullough, B.F., “Importance of Concrete Temperature Control During Concrete Pavement Construction in Hot Weather Conditions”, Transportation Research Record 1813, 2002, pp 3-10.

Westergaard, H.M., “Stresses in Concrete Pavements Computed by Theoretical Analysis”, Public Roads, 1927, pp 25-35.